Proceedings of the Seventh Fuel and Combustion Conference of Iran
Feb. 13 - 14, 2018, Sharif University of Technology, Tehran, Iran
FCCI-2018-1041

Mathematical Investigation of Oscillating Flame in Non-Premixed Counterflow Combustion of Particles

Gholamreza Shahriari Moghadam[a], Hesam Moghadasi*[a], Navid Malekian[a], Mehdi Bidabadi[a]

[a] *School of Mechanical Engineering, Department of Energy Conversion, Iran University of Science and Technology (IUST), Narmak, 16846-13114, Tehran, Iran*

*Email address(Corresponding author): hesam_moghadasi@mecheng.iust.ac.ir

Abstract
In this research, the influence of various effective dimensionless numbers on initiation of instability in combustion of organic particles is evaluated. A non-premixed counterflow combustion is considered assuming a thin region of vaporization where lycopodium particles are assumed as the solid fuel particles. It is assumed that particles as fuel and air as oxidizer move toward stagnation plane from two nozzles in the counterflow configuration. Particles initially vaporize in order to release a specific chemical gas which then enters the oxidation reaction process. To investigate oscillating characteristics of flame, governing equations are rewritten in dimensionless space-time coordinates. By solving these equations and combining them, a new expression is obtained. Also, by solving this equation, it is possible to predict initiation of instability in organic dust flame. According to the obtained results, by increasing Lewis number, threshold of instability happens earlier. Increasing wave number causes the instability boundary to go higher. It is also concluded that at a constant wave number, by increasing Zeldovich number, the onset of pulsating instability could occur with a smaller Lewis number.

Keywords: Non-Premixed Combustion, Counterflow, Vaporization, Instability

1. Introduction

Organic dust flame is associated with multi-phase combustion field in which interactions between particles and gaseous fuel affect flame characteristics. It is necessary to study all of the effective parameters on organic dust flame so as to have a complete view on this phenomenon. The Lewis number has a fundamental role in combustion of diffusion flames. A theoretical study aimed at understanding the basic mechanisms responsible for the onset of oscillations in diffusion flames is presented in Ref. [1]. This approach allows for non-unity Lewis numbers. They occur when the reactant diffusing against the stream is more completely consumed and the corresponding Lewis number is large enough.

More than power generation issues, micro-scale organic dusts have an extraordinary combustive behavior. Explosion occurs in most of the organic particles. Any solid substance that can be burnt in air will have the same behavior with the severity and velocity which increase with the degree of sub-division of the material. They have been a recognized threat to humans and properties for the recent years [2].

In last decades, a few researches have been done on organic dust combustion. Hence, fundamental information such as structure and movement of combustion zone in a dust particle cloud in a vertical duct is still ambiguous. Combustion of heterogeneous mixtures, including combustible and oxidizer particles is used in many engineering and safety fields. Combustion mechanisms of two-phase mixtures that deal with the combustion research of organic particles in geometries such as counterflow, are not fully understood so far [3-18].

Lycopodium is considered as the fuel particle in the current paper. Lycopodium has been known as a reference particle in organic dust combustion studies since being mono-size is a basic assumption in mathematical models [19-21].

Proust [22] focused on the initiation and propagation of flame in dust clouds to provide a more in-depth understanding of the incidence of thermal radiation and turbulence in dust explosion. Han et al. [23] experimentally analyzed the flame propagation mechanism and dust particles behavior in a vertical duct. Some parametric studies were conducted by Daou [24] to realize the effect of heat loss, preferential diffusion and reversibility of reaction. Up until 2009, there was no research addressing the recirculation effect in dust particles. Bidabadi et al. [25] analyzed this importance in a comprehensive manner. They developed a model to consider this effect in dust particles. Besides, Bidabadi and Rahbari [26] studied the influence of temperature alteration between particle and gas in a combustible mixture of homogeneously distributed volatile fuel particles. In another study, Rockwell and Rangwala [27] scrutinized a premixed flame in existence of a homogenous gas-phase reaction front. Haghiri and Bidabadi [28] examined the outcome of thermal radiation on the flame propagation throughout organic dust cloud.In another work Bidabadi et al. [29] investigated of effective dimensionless numbers on initiation of instability in combustion of moisty organic dust. Soltaninejad et al. [30] analyzed micro-organic dust combustion cogitating particles thermal resistance. In their model, it was presumed that gaseous fuel was formed as a result of particle pyrolysis.

In this work, a mathematical model is presented to study the instability of non-premixed counterflow combustion of particles. There are three instability mechanisms related with organic particles combustion, namely the hydrodynamic instability due to the density jump across the flame front, the diffusive-thermal instability induced by the disparities between mass and thermal diffusivities of the combustible mixture, and the last one is called acoustic instability.

2. Governing Equations

Counterflow geometry is very functional in the combustion science. Counterflow configuration is presumed so that organic particles come from $-\infty$ and move toward the stagnation plane and oxidizer comes from $+\infty$. Firstly, fuel particles vaporize to release a gaseous fuel with a certain chemical structure. Surface reactions will be neglected as well. Then, gaseous fuel will enter to the combustion process with oxidizer. The position of flame formation relies on initial conditions which can happen at the left or right side of stagnation plane. Altering the initial conditions will make a change in this position.

The structure of diffusion counterflow combustion of organic particles is illustrated in Figure 1 in a model having thin reaction and vaporization zones. Fuel particles in an asymptotic zone which is called vaporization front, suddenly vaporize and a gaseous fuel will be released. The gaseous fuel reacts with oxidizer flow in an asymptotic zone which is called flame front. The flame front position can be formed on the sides of the stagnation plane which relies on the initial conditions of the problem. As can be observed in Figure 1, the flame position is situated at the left side of the stagnation plane which also can be supposed in the right side as well.

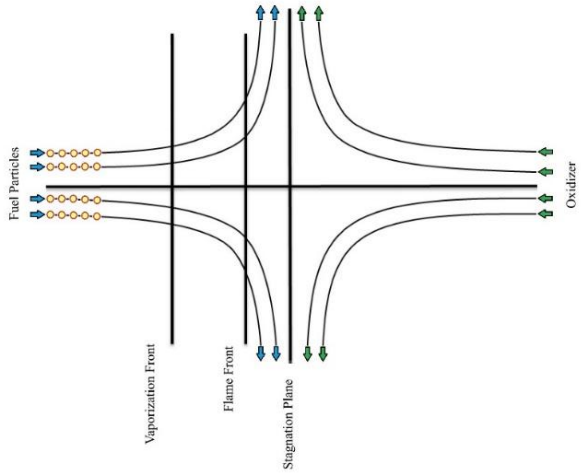

Figure 1 Structure of diffusion counterflow combustion

In the organic particles combustion, the vaporization rate defined as produced gaseous fuel mass per unit volume and time, is a controller parameter of combustion process. In this research, vaporization rate is considered as:

$$\omega_v = \frac{Y_s H(T - T_v)}{\tau_{vap}} \quad (1)$$

Also, τ_{vap} is characteristic time of vaporization, T and T_v are fuel and vaporization temperatures and H is Heaviside function.

Another factor which controls the combustion process is Lewis number. The Lewis number is defined as ratio of heat diffusion to mass diffusion, thus:

$$Le = \frac{\lambda}{\rho C D} \quad (2)$$

Where λ, ρ, C and D are conductivity, density, specific heat and mass diffusive coefficient, respectively.

Chemical kinetic is assumed as a general one-stage reaction. Furthermore, velocity field is considered as $(u,v) = (-aX,aY)$ where u and v are velocities in X and Y directions.

2.1 Mass Conservation of Solid Fuel

If the solid particles diffusion is negligible and with this assumption which solid particles don't have any reactions together, the mass conservation of solid fuel particles is written as:

$$\frac{\partial Y_s}{\partial t} - aX\frac{\partial Y_s}{\partial X} = -\omega_v \quad (3)$$

Where Y_s is mass fraction of solid particles and ω_v is the vaporization rate which has been defined in Eq. (1), previously.

2.2 Mass Conservation of Gaseous Fuel

$$\frac{\partial Y_F}{\partial t} - aX\frac{\partial Y_F}{\partial X} = D_F\frac{\partial^2 Y_F}{\partial X^2} - \frac{\omega_F}{\rho} + \omega_v \quad (4)$$

Where D_F and Y_F are mass diffusivity of fuel and mass fraction of gaseous fuel, respectively. ω_F is the rate of chemical reaction which follows the Arihinious rule and is in the first order relative to fuel and oxidizer. It is define as:

$$\omega_F = B\, Y_i\, exp\left(-\frac{E}{RT}\right) \quad (5)$$

2.3 Mass Conservation of Oxidizer

$$\frac{\partial Y_o}{\partial t} - aX\frac{\partial Y_O}{\partial X} = D_O\frac{\partial^2 Y_O}{\partial X^2} - \vartheta\frac{\omega_F}{\rho} \quad (6)$$

In the above equation, D_O, Y_O and ϑ are oxidizer mass diffusivity, oxidizer mass fraction and stoichiometric mass ratio of oxygen to fuel, respectively.

2.4 Energy Conservation of Mixture

$$\frac{\partial T}{\partial t} - aX\frac{\partial T}{\partial X} = D_T\frac{\partial^2 T}{\partial X^2} + \omega_F\frac{Q}{C} - \omega_v\frac{Q_v}{C} \quad (7)$$

Where Q is the heat released per unit of consumed fuel mass, Q_v is the latent vaporization heat of particles. Also, D_T is thermal diffusivity and C is specific heat of mixture which is obtained from combination of gaseous phase specific heat and solid particles specific heat as below:

$$C = C_a + \frac{4}{3}\pi r_P^3 n_P\frac{\rho_P}{\rho}C_P \quad (8)$$

Where ρ_P is the solid particle density and n_P shows the number of particles per unit of volume. Thus:

$$\rho = \rho_a + \frac{4}{3}\pi r_P^3 n_P \rho_P \tag{9}$$

2.5 Dimensionless Parameters

For dimensionless form of equations, some variables are defined as below.

$$\begin{aligned} x &= \sqrt{\frac{\rho C a}{\lambda}} X \\ y_s &= \frac{Y_s}{Y_{F-\infty}} \\ y_F &= \frac{Y_F}{Y_{F-\infty}} \\ y_o &= \frac{Y_O}{\vartheta Y_{F-\infty}} \\ \theta &= \frac{C}{Q}\frac{(T - T_\infty)}{Y_{F-\infty}} \end{aligned} \tag{10}$$

$Y_{F-\infty}$is the mass fraction of fuel at the position $-\infty$ where the fuel is coming from the fuel nozzle. Here, T_∞ represents the temperature in the outlets of nozzles. By substituting dimensionless parameters into the conservation equations, dimensionless conservation equations will be achieved.

3. Instability Investigation

In this section, the perturbed structure of flame propagation through the two-phase mixture is investigated. The main intention of this analysis is to bring insight about the fact that the unsteady conservation laws governing on organic particles combustion affect the stability boundary. For this end, governing conservation Eqs. (4), (6), and (7) are rewritten in the perturbed coordinates.

The flame front normal propagation in the main coordinate system (x, y, t) is as follows:

$$(\xi,\eta,\tau) = \left\{\left(x - x_{df}(y,t)\right)\frac{U_{x_f}}{D_T}, y\frac{U_{x_f}}{D_T}, t\frac{U_{x_f}{}^2}{D_T}\right\} \tag{11}$$

$$x_{df}(y,t) = -U_{x_f} t + \varepsilon\phi(y,t) \tag{12}$$

$$\phi(y,t) = \frac{D_T}{U_{x_f}}\Phi(\eta,\tau) \tag{13}$$

$$(\eta,\tau) = exp(\omega\tau)[cos(k\eta) + i\, sin(k\eta)] \tag{14}$$

By introducing the new dimensionless variables to the previous conservation equations system, the new perturbed system is obtained as:

$$\frac{\partial y_s}{\partial \tau} + \left[1 - \varepsilon\frac{\partial\Phi(\eta,\tau)}{\partial\tau}\right]\frac{\partial y_s}{\partial\xi} = -\widehat{\omega}_v \tag{15}$$

$$\frac{\partial y_F}{\partial \tau} + \left[1 - \varepsilon\frac{\partial\Phi(\eta,\tau)}{\partial\tau}\right]\frac{\partial y_F}{\partial\xi} = \frac{1}{Le_F}\Delta y_F + \widehat{\omega}_v - \widehat{\omega}_F \tag{16}$$

$$\frac{\partial y_O}{\partial \tau} + \left[1 - \varepsilon\frac{\partial\Phi(\eta,\tau)}{\partial\tau}\right]\frac{\partial y_O}{\partial\xi} = \frac{1}{Le_O}\Delta y_O - \widehat{\omega}_F \tag{17}$$

$$\frac{\partial \theta}{\partial \tau} + \left[1 - \varepsilon\frac{\partial\Phi(\eta,\tau)}{\partial\tau}\right]\frac{\partial \theta}{\partial\xi} = \Delta\theta - \widehat{\omega}_v + \widehat{\omega}_F \tag{18}$$

The Laplacian Δ also possesses the form shown below:

$$\Delta = \frac{\partial^2}{\partial\xi^2} + \left(\frac{\partial}{\partial\eta} - \varepsilon\frac{\partial\Phi}{\partial\eta}\frac{\partial}{\partial\xi}\right)^2 \tag{19}$$

In order to achieve transient solutions for conservation equations, small perturbations method ($\varepsilon << 1$) is used. All variables are written as the sum of the steady state solution and a small harmonic perturbation. Fuel mass fraction, oxidizer mass fraction and temperature distributions are achieved in each zone.

$$\theta = \bar{\theta}(\xi) + \varepsilon\Phi(\eta,\tau)\tilde{\theta}(\xi) + O(\varepsilon^2) \tag{20}$$

$$y_F = \bar{y}_F(\xi) + \varepsilon\Phi(\eta,\tau)\tilde{y}_F(\xi) + O(\varepsilon^2) \tag{21}$$

$$y_O = \bar{y}_O(\xi) + \varepsilon\Phi(\eta,\tau)\tilde{y}_O(\xi) + O(\varepsilon^2) \tag{22}$$

The first terms on the RHS of Eqs. (20)-(22) correspond to the steady state flame structure, which are mentioned in the previous sentences. By assuming $\varepsilon << 1$, it is possible to derive linearized perturbation expressions for θ, y_F and y_O. By substituting Eqs. (20)-(22) in Eqs. (16)-(18) respectively, one can write:

$$\tilde{\theta}(\omega + k^2) + \frac{\partial\tilde{\theta}}{\partial\xi} - \frac{\partial\tilde{\theta}^2}{\partial\xi^2} = (\omega + k^2)\frac{\partial\bar{\theta}}{\partial\xi} - \tilde{\omega}_v + \tilde{\omega}_F \tag{23}$$

$$\begin{aligned} \tilde{y}_F\left(\omega + \frac{k^2}{Le_F}\right) + \frac{\partial\tilde{y}_F}{\partial\xi} - \frac{1}{Le_F}\frac{\partial^2\tilde{y}_F}{\partial\xi^2} \\ = \left(\omega + \frac{k^2}{Le_F}\right)\frac{\partial\bar{y}_F}{\partial\xi} + \tilde{\omega}_v - \tilde{\omega}_F \end{aligned} \tag{24}$$

$$\begin{aligned} \tilde{y}_O\left(\omega + \frac{k^2}{Le_O}\right) + \frac{\partial\tilde{y}_O}{\partial\xi} - \frac{1}{Le_O}\frac{\partial^2\tilde{y}_O}{\partial\xi^2} \\ = \left(\omega + \frac{k^2}{Le}\right)\frac{\partial\bar{y}_O}{\partial\xi} - \tilde{\omega}_F \end{aligned} \tag{25}$$

Where $\tilde{\omega}_v$ and $\tilde{\omega}_F$ are oscillating vaporization and reaction rates, respectively. At ξ_{vap} the fact that vaporization of organic particles does not initiate from a fixed point, and it is a remarkable reason for observing pulsating flame propagation thought two-phase mixture with volatile particles. The oscillation of vaporization position within the flame structure is as follows:

$$\tilde{\xi}_{vap} = \frac{-\tilde{\theta}\big|_{\xi=\xi_{vap}}}{\frac{\partial\bar{\theta}}{\partial\xi}\Big|_{\xi=\xi_{vap}}} \tag{26}$$

3.1 Boundary Conditions

According to the proposed geometry, boundary conditions for temperature, fuel mass fraction and oxidizer mass fraction perturbations in different boundaries are expressed as:

- $\boldsymbol{\xi \to \pm\infty}$

In this position, boundary conditions are written as:

$$\begin{aligned} \tilde{\theta} &= 0 \\ \tilde{y}_s &= 0 \\ \tilde{y}_i &= 0 \end{aligned} \tag{27}$$

- $\boldsymbol{\xi = \xi_{vap}}$

In this position, according to heat, gaseous fuel and oxidizer diffusions, continuity in temperature, mass fractions of gaseous fuel and oxidizer, as well as their derivations are stated as:

$$\begin{aligned}&\left[\tilde{\theta}\right]_{\xi=\xi_{vap}}=0\\&\left[\tilde{y}_i\right]_{\xi=\xi_{vap}}=0\\&\left[\frac{d\tilde{\theta}}{d\xi}\right]_{\xi=\xi_{vap}}=0\\&\left[\frac{d\tilde{y}_i}{d\xi}\right]_{\xi=\xi_{vap}}=0\end{aligned}\qquad(28)$$

- $\boldsymbol{\xi=\xi_{flame}}$

In this position, boundary and matching conditions are presented as:

$$\begin{aligned}&\left[\tilde{y}_i\right]=0\\&\left[\tilde{\theta}\right]=0\\&\left[\frac{\partial\tilde{\theta}}{\partial\xi}+\frac{1}{Le_i}\frac{\partial\tilde{y}_i}{\partial\xi}\right]=0\end{aligned}\qquad(29)$$

The following expansion is presumed such that $\tilde{\theta}_o(\xi)$ and $\tilde{\theta}_1(\xi)$ are the first and second terms of $\tilde{\theta}(\xi)$ expansion on $\frac{1}{Ze}$, respectively. Is should be said that Zeldovich number is of large value.

$$\tilde{\theta}(\xi)=\tilde{\theta}_o(\xi)+\left(\frac{1}{Ze}\right)\tilde{\theta}_1(\xi)+O\left(\frac{1}{Ze^2}\right)\qquad(30)$$

$$\tilde{y}_i=(\tilde{y}_i)_0+\left(\frac{1}{Ze}\right)(\tilde{y}_i)_0+O\left(\frac{1}{Ze^2}\right)\qquad(31)$$

In the current paper, organic particles are considered to release a certain gaseous fuel and then enter the combustion process. Hence, the relationship proposed by Sivashinsky [31] for gaseous fuels is utilized in order to relate $\tilde{\theta}_o(\xi)$ with $\tilde{\theta}_1(\xi)$.

$$\left(\frac{\partial\tilde{\theta}_0(\xi)}{\partial\xi}\right)_{0^-}=\frac{1}{2}\left(\tilde{\theta}_1(\xi)\right)_0\qquad(32)$$

3.2 Solutions

In this section, perturbed equations are solved regarding to the mentioned boundary conditions. Then, temperature, gaseous fuel mass fraction and oxidizer mass fraction fields are obtained in various zones of flame structure which are considered as:

$$R_1:\{\xi|\xi_f-\varepsilon<\xi<\xi_f\}\qquad(33)$$

$$R_2:\{\xi|\,\xi_f<\xi<\xi_f+\varepsilon\}\qquad(34)$$

3.2.1 Distribution of Gaseous Fuel Mass Fraction

Conservation equation of gaseous fuel mass in different zones is as follows:

- **In $\boldsymbol{R_1}$**

$$\begin{aligned}&\tilde{y}_F(\xi)\\&=F\left[\operatorname{erf}\left(\frac{1}{2}\left(\sqrt{\frac{Le_F}{2}}(2\xi+1)-E\right)\right)\exp\left(\left(\frac{Le_F}{2}\right.\right.\right.\\&\left.-\sqrt{\frac{Le_F}{2}}\mathrm{E}\right)\xi+\frac{1}{2Le_F}\left(\sqrt{\frac{Le_F}{2}}E-\frac{Le_F}{2}\right)^2\\&-\operatorname{erf}\left(\frac{\mathrm{P}+Le_F\xi+\frac{Le_F}{2}}{2\sqrt{\frac{Le_F}{2}}}\right)\exp\left(\left(\sqrt{\frac{Le_F}{2}}\mathrm{E}+\frac{Le_F}{2}\right)x\right.\\&+\frac{\left(\omega+\frac{k^2}{Le_F}\right)}{2}+\frac{1}{2}\sqrt{\frac{Le_F}{2}}\mathrm{E}+\frac{\frac{Le_F}{2}}{2}\Big)\\&+\operatorname{erf}\left(\frac{P+\frac{3Le_F}{2}}{2\sqrt{\frac{Le_F}{2}}}\right)\exp\left(\left(\sqrt{\frac{Le_F}{2}}\mathrm{E}+\frac{Le_F}{2}\right)\xi+\frac{\left(\omega+\frac{k^2}{Le_F}\right)}{2}\right.\\&+\frac{1}{2}\sqrt{\frac{Le_F}{2}}\mathrm{E}+\frac{\frac{Le_F}{2}}{2}\Big)+\operatorname{erf}\left(\frac{1}{2}(\mathrm{E}\right.\\&\left.\left.-3\sqrt{\frac{Le_F}{2}}\right)\right)\exp\left(\left(11-\sqrt{\frac{Le_F}{2}}\mathrm{E}\right)\xi\right.\\&\left.\left.+\frac{1}{2Le_F}\left(\sqrt{\frac{Le_F}{2}}\mathrm{E}-\frac{Le_F}{2}\right)^2\right)\right]\\&+C_1\exp\left(\left(\frac{Le_F}{2}-\sqrt{\frac{Le_F}{2}}\mathrm{E}\right)\xi\right)\\&+C_2\exp\left(\sqrt{\frac{Le_F}{2}}\mathrm{E}+\frac{Le_F}{2}\right)\xi\Big)\end{aligned}\qquad(35)$$

In which F, E and P are introduced as below:

$$F=\frac{y_{Fv}\left(\omega+\frac{k^2}{Le_F}\right)\sqrt{2}}{\left(\operatorname{erf}\left(\frac{\xi_v}{\sqrt{\frac{2}{Le_F}}}\right)-\operatorname{erf}\left(\frac{\xi_f}{\sqrt{\frac{2}{Le_F}}}\right)\right)2\sqrt{2\left(\omega+\frac{k^2}{Le_F}\right)+\frac{Le_F}{2}}}\qquad(36)$$

$$E=\sqrt{2\left(\omega+\frac{k^2}{Le_F}\right)+\frac{Le_F}{2}}\qquad(37)$$

$$P=\sqrt{Le_F\left(\omega+\frac{k^2}{Le_F}\right)+\left(\frac{Le_F}{2}\right)^2}\qquad(38)$$

- **In $\boldsymbol{R_2}$**

$$\tilde{y}_F(\xi)=0\qquad(39)$$

3.2.2 Distribution of Oxidizer Mass Fraction

Conservation equation of oxidizer mass in different zones is as follows:

- **In $\boldsymbol{R_1}$**

$$\tilde{y}_O(\xi)=0\qquad(40)$$

- **In $\boldsymbol{R_2}$**

$$
\begin{aligned}
&\tilde{y}_o(\xi) \\
&= N'\Bigg[\mathrm{erf}\Bigg(\frac{1}{2}\Big(\sqrt{\frac{Le_o}{2}}(2\xi+1) \\
&-\sqrt{2a+\frac{Le_o}{2}}\Bigg)\exp\Big(\Big(\frac{Le_o}{2}-\sqrt{\frac{Le_o}{2}}\sqrt{2a+\frac{Le_o}{2}}\Big)\xi \\
&+\frac{1}{2Le_o}\Bigg(\sqrt{\frac{Le_o}{2}}N-\frac{Le_o}{2}\Bigg)^2 \\
&-\mathrm{erf}\Big(\frac{I+Le_F\xi+\frac{Le_o}{2}}{2\sqrt{\frac{Le_o}{2}}}\Big)\exp\Big(\Big(\sqrt{\frac{Le_o}{2}}\mathrm{N}+\frac{Le_o}{2}\Big)x\xi \\
&+\frac{\left(\omega+\frac{k^2}{Le_o}\right)}{2}+\frac{1}{2}\sqrt{\frac{Le_o}{2}}\mathrm{N}+\frac{\frac{Le_o}{2}}{2}\Big) \\
&+\mathrm{erf}\Big(\frac{I+\frac{3Le_o}{2}}{2\sqrt{\frac{Le_o}{2}}}\Big)\exp\Big(\Big(\sqrt{\frac{Le_o}{2}}\sqrt{2a+\frac{Le_o}{2}}+\frac{Le_o}{2}\Big)\xi \\
&+\frac{\left(\omega+\frac{k^2}{Le_o}\right)}{2}+\frac{1}{2}\sqrt{\frac{Le_o}{2}}\mathrm{N}+\frac{\frac{Le_o}{2}}{2}\Big)+\mathrm{erf}\Big(\frac{1}{2}(\mathrm{N} \\
&-3\sqrt{\frac{Le_o}{2}}\Big)\Big)\exp\Bigg(\Bigg(11-\sqrt{\frac{Le_o}{2}}\mathrm{N}\Bigg)\xi \\
&+\frac{1}{2Le_o}\Bigg(\sqrt{\frac{Le_o}{2}}\mathrm{N}-\frac{Le_o}{2}\Bigg)^2\Bigg)\Bigg] \\
&+C_1\exp\Bigg(\Bigg(\frac{Le_o}{2}-\sqrt{\frac{Le_o}{2}}\mathrm{N}\Bigg)\xi\Bigg) \\
&+C_2\exp\Bigg(\sqrt{\frac{Le_o}{2}}\mathrm{N}+\frac{Le_o}{2}\Big)\xi\Bigg)
\end{aligned}
\tag{41}
$$

In which N, N' and Y are introduced as below:

$$N=\sqrt{2\left(\omega+\frac{k^2}{Le_o}\right)+\frac{Le_o}{2}} \tag{42}$$

$$N'=\frac{\left(\omega+\frac{k^2}{Le_o}\right)\alpha\sqrt{2}}{\left(1-\mathrm{erf}\left(\frac{\xi_f}{\sqrt{\frac{2}{Le_o}}}\right)\right)2T} \tag{43}$$

$$I=\sqrt{Le_o\left(\omega+\frac{k^2}{Le_o}\right)+\left(\frac{Le_o}{2}\right)^2} \tag{44}$$

3.2.3 Distribution of Temperature

Conservation equation of temperature in different zones is as follows:

- **In R_1**

$$
\begin{aligned}
\tilde{\theta}_0(\xi) = \mathrm{A}\Bigg[&\Big(-\mathrm{erf}\Big(\frac{\mathrm{B}-2\xi-1}{2\sqrt{2}}\Big)\exp\Big[\frac{1}{8}(B \\
&-1)(\mathrm{B}-4\xi-1)\Big] \\
&+\mathrm{erf}\Big(\frac{\mathrm{B}-3}{2\sqrt{2}}\Big)\exp\Big[\frac{1}{8}(\mathrm{B} \\
&-1)(\mathrm{B}-4\xi-1)\Big] \\
&-\exp\Big[\frac{1}{8}(\mathrm{B}+1)\big(\sqrt{4a+1} \\
&+4\xi+1\big)\Big]\mathrm{erf}\Big(\frac{\mathrm{B}+2\xi+1}{2\sqrt{2}}\Big) \\
&+\mathrm{erf}\Big(\frac{\mathrm{B}+3}{2\sqrt{2}}\Big)\exp\Big[\frac{1}{8}(\mathrm{B} \\
&+1)(\mathrm{B}+4\xi+1)\Big]\Bigg] \\
&+C_1\exp\Big(-\frac{1}{2}(\mathrm{B}-1)\xi\Big) \\
&+C_2\exp\Big(\frac{1}{2}(\mathrm{B}+1)\xi\Big)
\end{aligned}
\tag{45}
$$

In which A and B are introduced as below:

$$A=\frac{(\omega+k^2)\sqrt{\frac{2}{8a+2}}(\bar{\theta}_f-\bar{\theta}_v)}{\left(\mathrm{erf}(\frac{\xi_f}{\sqrt{2}})-\mathrm{erf}(\frac{\xi_v}{\sqrt{2}})\right)} \tag{46}$$

$$B=\left(\sqrt{4(\omega+k^2)+1}\right) \tag{47}$$

- **In R_2**

$$
\begin{aligned}
\tilde{\theta}_0(\xi) = G\Bigg[&\Big(-\mathrm{erf}\Big(\frac{B-2\xi-1}{2\sqrt{2}}\Big)\exp\Big[\frac{1}{8}(\mathrm{B} \\
&-1)(\mathrm{B}-4\xi-1)\Big] \\
&+\mathrm{erf}\Big(\frac{B-3}{2\sqrt{2}}\Big)\exp\Big[\frac{1}{8}(\mathrm{B} \\
&-1)(\mathrm{B}-4\xi-1)\Big] \\
&-\exp\Big[\frac{1}{8}(\mathrm{B}+1)\big(\sqrt{4a+1} \\
&+4\xi \\
&+1\big)\Big]\mathrm{erf}\Big(\frac{B+2\xi+1}{2\sqrt{2}}\Big) \\
&+\mathrm{erf}\Big(\frac{\mathrm{B}+3}{2\sqrt{2}}\Big)\exp\Big[\frac{1}{8}(\mathrm{B} \\
&+1)(\mathrm{B}+4\xi+1)\Big]\Bigg] \\
&+C_1\exp\Big(-\frac{1}{2}(\mathrm{B}-1)\xi\Big) \\
&+C_2\exp\Big(\frac{1}{2}(\mathrm{B}+1)\xi\Big)
\end{aligned}
\tag{48}
$$

In which

$$G=\frac{(\omega+k^2)\sqrt{\frac{2}{8a+2}}\,\bar{\theta}_f}{\left(\mathrm{erf}\left(\frac{\xi_v}{\sqrt{2}}\right)-1\right)} \tag{49}$$

4. Results and Discussion

In this section, the results obtained from solutions of the spreading flame in organic particle cloud are classified into two parts. In the first part, the instability boundary for a planar flame propagating in the two-phase mixture is determined, and in the second part, the instability of the wrinkled flame is

taken into account. As mentioned previously, the released gas from lycopodium particles is considered to be methane [32-34] which its properties are presented in Table1.

Table 1 Lycopodium Properties [32-34]

Property	Value
ρ_P	$1000\ \frac{kg}{m^3}$
ρ_a	$1.164\ \frac{kg}{m^3}$
C_P	$5.677688\ \frac{kJ}{kg \cdot K}$
C_a	$1.00416\ \frac{kJ}{kg \cdot K}$
Q	$64895.4\ \frac{kJ}{kg}$

Furthermore, the combustion reaction is denoted as:
$CH_4 + 2(O_2 + 3.76N_2) \longrightarrow CO_2 + 2H_2O + 7.52N_2$

4.1 Delimitation of Instability Boundary in Planar Flame ($k = 0$)

As stated previously, numerous studies have not been conducted on the subject of instability in the combustion of dust particles cloud.
In fact, no mathematical formula has been proposed that predicts the onset of instability for flame propagating through organic particles cloud.
In Figure 2, the instability boundaries of the planar flame acquired through the present model in two cases of $\theta_v = 0.1$ and $\theta_v = 0.15$ are demonstrated. As Figure 2 shows, by increasing Lewis number, critical Zeldovich number experiences a decreasing trend. Also, for larger values of θ_v, the curves are located at higher levels.

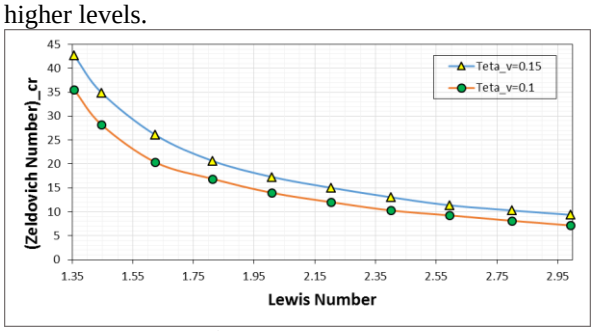

Figure 2 Variations of critical Zeldovich number versus Lewis number for two different θ_v

Figure 3 shows the frequency of oscillations at instability threshold for planar flame in the two-phase mixture, for the conditions outlined in Figure 2. By an increase in Lewis number, at a constant θ_v, frequency of the oscillations decreases. Also, an increase in θ_v, at a fixed Lewis number, leads to a rise in frequency of oscillations.

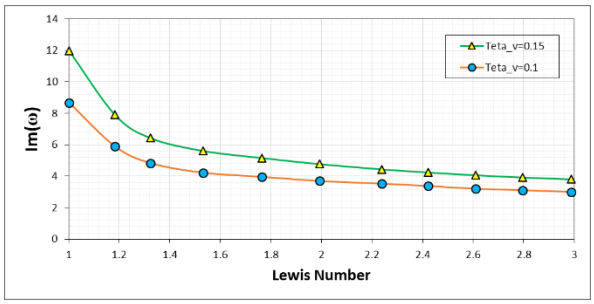

Figure 3 Variations of oscillation frequency versus Lewis number for two different θ_v

4.2 Delimitation of Instability Boundary in Wrinkled Flame ($k \neq 0$)

In this part, the effect of wave number variations on the instability boundary in the wrinkled flame front are reviewed. It should be noted that a non-zero wave number ($k \neq 0$) means wrinkled flame front.
Defining the oscillating instability boundary on the basis of critical Zeldovich number against change of wave number at a constant Lewis number, has been presented in Figure 4. As this figure shows, by increasing wave number at a fixed value of Lewis number, oscillating instability boundary rises. The noteworthy point in this figure is the sharp reduction of the critical Zeldovich number versus the increase of the Lewis number at a constant wave number which is circumstance that enhances the possibility of starting the oscillating instability in a wrinkled flame front.

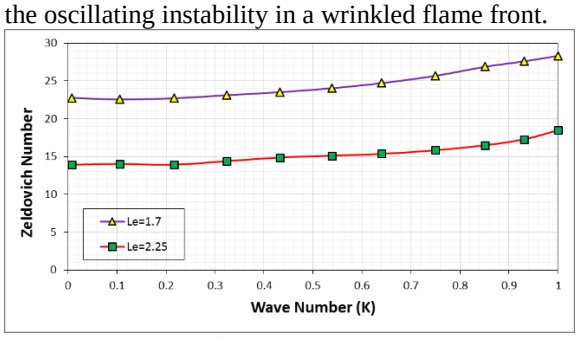

Figure 4 Variations of critical Zeldovich number versus wave number for two different Lewis numbers

Oscillations Frequency of the wrinkled flame propagating through the organic particle cloud is shown in Figure 5 for the conditions of Figure 4. By increasing wave number at a fixed Lewis number, frequency of the starting oscillations increases. Also, an increase in Lewis number at a constant wave number leads to a decrease in the frequency of oscillations at the onset of instability.

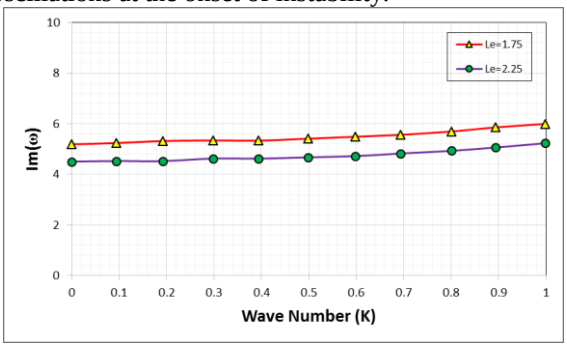

Figure 5 Variations of oscillation frequency versus wave number for two different Lewis numbers

Delimitation of pulsating instability boundary of the wrinkled flame in the $Le_{cr} - k$ plane, for a constant Zeldovich number, is illustrated in Figure 6. Increasing wave number causes the instability boundary to go higher, which is defined by the critical Lewis number in this figure. It is also concluded from this figure that at a constant k, by increasing Zeldovich number, the onset of pulsating instability could occur with a smaller Lewis number.

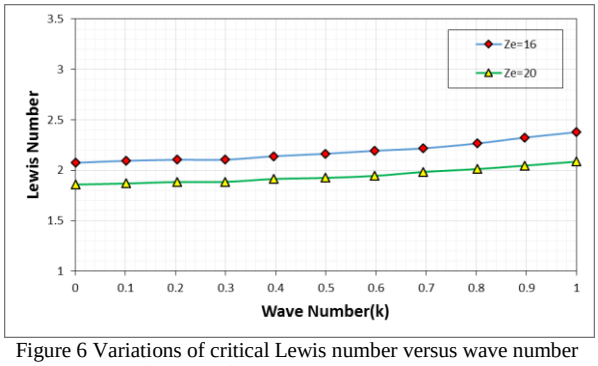

Figure 6 Variations of critical Lewis number versus wave number for two different Zeldovich numbers

5. Conclusion

In this paper, the combustion of organic particles in counterflow configuration was considered assuming asymptotic zones for vaporization and reaction. Assuming particles to vaporize first to produce a specific chemical gas. To investigate oscillating characteristics of flame, gaseous fuel mass fraction, oxidizer mass fraction and mixture energy equation are rewritten in dimensionless space-time coordinates. By solving these equations, it is possible to predict initiation of instability in organic dust flame. According to the obtained results, by increasing Lewis number, threshold of instability happens earlier. Increasing wave number causes the instability boundary to go higher. It is also concluded that at a constant wave number, by increasing Zeldovich number, the onset of pulsating instability could occur with a smaller Lewis number.

Nomenclature

a	Strain rate
C_a	Heat capacity of gaseous fuel
C_P	Heat capacity of solid particle
D_F	Mass diffusivity of gaseous fuel
D_O	Mass diffusivity of oxidizer
D_T	Thermal conductivity
H	Heaviside function
k	Wave number
Le	Lewis number
m	Molecular weight of mixture
m_f	Molecular weight of fuel
m_O	Molecular weight of oxidizer
n_P	Number of particles per unit volume
Q	Heat of reaction
Q_v	Latent heat of particles vaporization
R	Universal gas constant
r	Radius
T	Temperature
T_v	Vaporization temperature
Y_F	Mass fraction of gaseous fuel
$Y_{F-\infty}$	Mass fraction of fuel at a distance of $-\infty$
Y_O	Mass fraction of oxidizer
Y_s	Mass fraction of solid fuel

Greek Letters

α	Initial mass fraction oxidizer
η	Dimensionless position
θ	Dimensionless temperature
ϑ	Stoichiometric mass ratio of oxidizer to fuel
ξ	Dimensionless position
ρ	Density
ρ_P	Density of solid particle
τ	Dimensionless time
τ_v	Characteristic time of vaporization
v_F	Stoichiometric coefficient of fuel
v_O	Stoichiometric coefficient of oxidizer
v_P	Stoichiometric coefficient of products
ω_F	Rate of the chemical kinetics
ω_v	Vaporization rate of particles

References

[1] Leu, J.H., 2010. Biomass power generation through direct integration of updraft gasifier and Stirling engine combustion system. Advances in Mechanical Engineering, 2, p.256746.

[2] Han, O.S., Yashima, M., Matsuda, T., Matsui, H., Miyake, A. and Ogawa, T., 2000. Behavior of flames propagating through lycopodium dust clouds in a vertical duct. Journal of Loss Prevention in the Process Industries, 13(6), pp.449-457.

[3] Malekian, N., Moghadasi, H., Bidabadi, M. and Moghadam, G.S., 2017 Efficiency Analysis in a Furnace Regenerator Using Lycopodium Particles. The 25th Annual International Conference on Mechanical Engineering ISME2017, Tarbiat Modares university, Tehran, Iran.

[4] Moghadasi, H., Malekian, N., Bidabadi, M. and Moghadam, G.S., 2017 An analytical modeling of

particles thermal resistance in pre-mixed organic dust (Lycopodium) combustion. The 25th Annual International Conference on Mechanical Engineering ISME2017, Tarbiat Modares university, Tehran, Iran.

[5] Afzalabadi, A., Poorfar, A.K., Bidabadi, M., Moghadasi, H., Hochgreb, S., Rahbari, A. and Dubois, C., 2017. Study on hybrid combustion of aero-suspensions of boron-aluminum powders in a quiescent reaction medium. Journal of Loss Prevention in the Process Industries, 49, pp.645-651.

[6] Bidabadi, M., Ramezanpour, M., Khoeini Poorfar, A., Monteiro, E. and Rouboa, A., 2016. Mathematical modeling of a Non-Premixed organic Dust flame in a Counterflow configuration. Energy & Fuels, 30(11), pp.9772-9782.

[7] Eckhoff, Rolf K. Dust explosions in the process industries: identification, assessment and control of dust hazards. Gulf professional publishing, 2003.

[8] Serio, Michael A., Erik Kroo, and Marek A. Wójtowicz. "Biomass pyrolysis for distributed energy generation." Prepr. Pap.-Am. Chem. Soc., Div. Fuel Chem48, no. 2 (2003): 584.

[9] Cashdollar, Kenneth L., and Isaac A. Zlochower. "Explosion temperatures and pressures of metals and other elemental dust clouds." Journal of Loss Prevention in the Process Industries 20, no. 4 (2007): 337-348.

[10] Broumand, Mohsen, and Mehdi Bidabadi. "Modeling combustion of micron-sized iron dust particles during flame propagation in a vertical duct." Fire Safety Journal 59 (2013): 88-93.

[11] Joseph, Giby, and CSB Hazard Investigation Team. "Combustible dusts: A serious industrial hazard." Journal of hazardous materials 142, no. 3 (2007): 589-591.

[12] Cashdollar, K.L., 2000. Overview of dust explosibility characteristics. Journal of Loss Prevention in the Process Industries, 13(3), pp.183-199.

[13] Seshadri, K. and Trevino, C., 1989. The influence of the Lewis numbers of the reactants on the asymptotic structure of counterflow and stagnant diffusion flames. Combustion science and technology, 64(4-6), pp.243-261.

[14] Dvorjetski, A. and Greenberg, J.B., 2000. Influence of non-unity Lewis numbers and droplet loading on the extinction of counter-flow spray diffusion flames. Proceedings of the Combustion Institute, 28(1), pp.1047-1054.

[15] Linan, A., 1974. The asymptotic structure of counterflow diffusion flames for large activation energies. Acta Astronautica, 1(7), pp.1007-1039.

[16] Wang, L., Liu, Z., Chen, S., Zheng, C. and Li, J., 2013. Physical and chemical effects of CO2 and H2O additives on counterflow diffusion flame burning methane. Energy & fuels, 27(12), pp.7602-7611.

[17] Ghoddoussi, R., 2005. An Investigation on Thermal Characteristics of Premixed Counterflow Flames Using Micro-thermocouples (Doctoral dissertation).

[18] Ren, J., Xie, C., Guo, X., Qin, Z., Lin, J.Y. and Li, Z., 2014. Combustion characteristics of coal gangue under an atmosphere of coal mine methane. Energy & Fuels, 28(6), pp.3688-3695.

[19] Mason, W.E. and Wilson, M.J.G., 1967. Laminar flames of lycopodium dust in air. Combustion and Flame, 11(3), pp.195-200.

[20] Bidabadi, Mehdi, Mohammad Rastegar Moghaddam, Seyed Alireza Mostafavi, Farzad Faraji Dizaji, and Hossein Beidaghy Dizaji. "An analytical model for pyrolysis of a single biomass particle." Journal of Central South University 22, no. 1 (2015): 350-359.

[21] Bidabadi, M., P. Aghajannezhad, M. Harati, E. Yaghoubi, and G. Shahriari. "Modeling random combustion of lycopodium particles and gas." International Journal of Spray and Combustion Dynamics 8, no. 2 (2016): 100-111.

[22] Proust, C., 2006. "Flame propagation and combustion in some dust-air mixtures". Journal of Loss Prevention in the Process Industries, 19(1), pp. 89-100.

[23] Han, O.S., 2009. "Flame Propagation Characteristics Through Suspended Combustible Particles in a Full-Scaled Duct". Korean Chemical Engineering Research, 47(5), pp. 572-579.

[24] J. Daou, strained premixed flames: Effect of heat-loss, preferential diffusion and reversibility of the reaction, Combust. Theory Model. 15 (4), (2011), 437-454.

[25] Bidabadi, M., Mostafavi, S.A., Dizaji, H.B. and Dizaji, F.F., 2013. Lycopodium dust flame characteristics considering char yield. Scientia Iranica. Transaction B, Mechanical Engineering, 20(6), p.1781.

[26] M. Bidabadi, A. Rahbari, Modeling combustion of lycopodium particles by considering the temperature difference between the gas and the particles, Combust. Expl. Shock Waves, 45, (2009), 278-285.

[27] Rockwell, Scott R., and Ali S. Rangwala. "Modeling of dust air flames." Fire Safety Journal 59 (2013): 22-29.

[28] Haghiri, A. and Bidabadi, M., 2012. Linear Stability Analysis of Pulsating Flame Propagation Through an Organic Dust Particle Cloud with Different Lewis Numbers and Heat Radiation Effects. Combustion Science and Technology, 184(3), pp.374-405.

[29] Bidabadi, M., Dizaji, F.F., Dizaji, H.B. and Ghahsareh, M.S., 2014. Investigation of effective dimensionless numbers on initiation of instability in combustion of moisty organic dust. Journal of Central South University, 21(1), pp.326-337.

[30] Soltaninejad, Mohammadamin, Farzad Faraji Dizaji, Hossein Beidaghy Dizaji, and Mehdi Bidabadi. "Micro-organic dust combustion considering particles thermal resistance." Journal of Central South University 22, no. 7 (2015): 2833-2840.

[31] Gutman, S. and Sivashinsky, G.I., 1990. The cellular nature of hydrodynamic flame instability. Physica D: Nonlinear Phenomena, 43(1), pp.129-139.

[32] Palmer, Kenneth Norman. Dust explosions and fires [by] KN Palmer. 1973.

[33] Bardon, M. F., and D. E. Fletcher. "Dust explosions." Science Progress (1933-) (1983): 459-473.

[34] Turns, Stephen R. An introduction to combustion. Vol. 287. New York: McGraw-hill, 1996.